Transactions, SMiRT-25
Charlotte, NC, USA, August 4-9, 2019
Division VII

Seismic Fragility based on Conditional Mean Spectra for Multiple Earthquake Scenarios

Ji-Hun Park[1], Seong-Ha Jeon[2], Wonho Park[2] and Beom Seok Kim [2]

[1] Professor, Division of Architecture &Urban Design, Incheon National University, Incheon, Republic of Korea (jhpark606@inu.ac.kr)
[2] Graduate Student, Department of Architecture, Incheon National University, Incheon, Republic of Korea

ABSTRACT

A methodology to assess seismic fragility of nuclear power plant (NPP) using conditional mean spectrum (CMS) considering multiple scenarios is proposed as an alternative of using a uniform hazard response spectrum (UHRS) where no single scenario is dominant. The proposed methodology utilizes multi-scenario conditional mean spectrum (MCMS) defined as a weighted average of different CMS of which each one corresponds to an individual scenario. Weighting factors are obtained from deaggregation of seismic hazards. As a validation example, seismic fragility assessment of a containment structure is performed using both UHRS and MCMS constructed for a NPP site. MCMS result in lower seismic response and higher HCLPF capacity compared to those from UHRS. The MCMS of which control frequency equals the dominant frequency of the evaluated structure results in the minimum randomness of spectral shape and achieves the maximum HCLPF among examined MCMS.

INTRODUCTION

UHRS has been used in order to define seismic hazards for seismic probabilistic risk assessment (SPRA) of NPP. Spectral accelerations in a UHRS have the same probability of exceedance for entire frequency range. However, each spectral acceleration of a UHRS is determined independently from one another without considering correlation. Therefore, it is unlikely that the entire frequency range has spectral accelerations corresponding to a UHRS. Thus, applying a UHRS to evaluate seismic analysis of a structure against a single event overestimate seismic risk. In order to overcome conservatism in UHRS, CMS was proposed by Baker (2011). CMS is constructed using correlation coefficients of epsilon between different frequencies and has the same spectral acceleration as a relevant UHRS at a specific control frequency. Also, CMS is dependent on assumed earthquake scenario since the epsilon is dependent on the mean spectral acceleration predicted based on a specific condition of the earthquake event. As a result, CMS represents more realistic spectral shape than the UHRS and tends to be lower as the frequency goes far from the control frequency. However, application of the CMS to SPRA of NPP is found limitedly in literature (Renault, 2011; Mohamed et al., 2015).

In this study, CMS are applied to SPRA of a NPP. The CMS is dependent on selection of the control frequency and earthquake scenario. Thus, influence of different control frequencies on seismic fragility is investigated. Regarding earthquake scenario, a case that there is no single dominant scenario exist and diverse scenarios are required to be considered in SPRA. A containment building structure modelled numerically. A UHRS at a NPP site and corresponding CMS are constructed considering frequency characteristics of the containment structure. Seismic fragility assessment is performed using a procedure of EPRI TR-103959 based on response spectrum analysis. Then, seismic fragility curves and HCLPF capacities are calculated and compared.

MODEL OF CONTAINMENT STRUCTURE

The containment structure of APR 1400 as shown in Figure 1(a) is adopted for case study. The structure is modelled in a beam-stick model composed of total 13 beam elements as shown in Figure 1(b). Only the outermost shell and dome are included in the numerical model. The natural frequency and modal mass participation factors are summarized in Table 1. The first two modes, of which natural frequencies are 4.10 and 12.25 Hz and mode shapes are illustrated in Figure 1(c) and (d), account for more than 90 %.

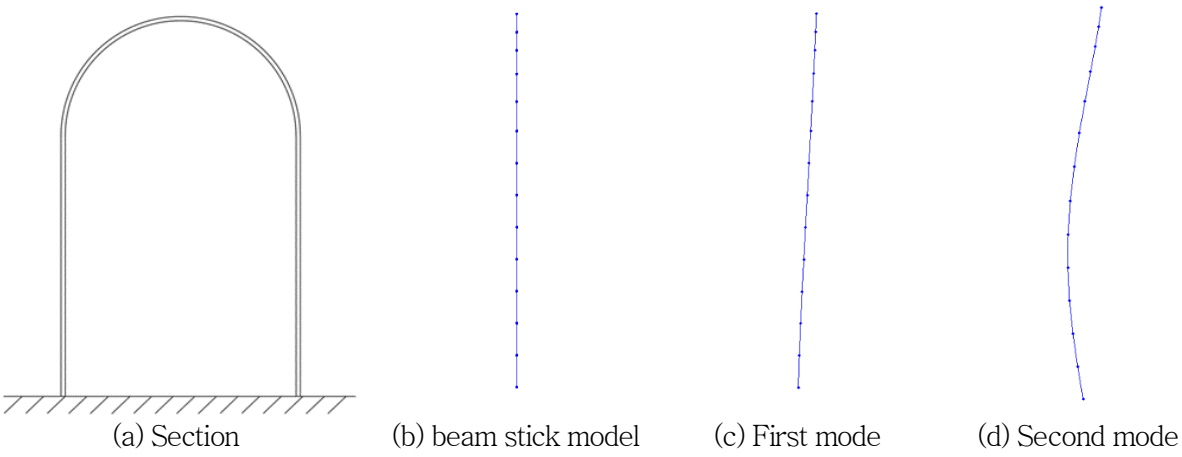

Figure 1. Containment structure and mode shapes

Table 1. Modal frequency and mass participation factor

Mode	Natural frequency (Cycle/sec)	Modal mass participation factor for translational degree of freedom	
		MASS(%)	SUM(%)
1	4.10	71.37	71.37
2	12.25	20.11	91.48
3	23.69	2.18	93.66
4	24.71	2.42	96.09
5	34.96	1.78	97.87
6	43.18	0.66	98.53
7	46.03	0.26	98.79

UNIFORM HAZARD RESPONSE SPECTRUM

A UHRS is constructed for a NPP site in the south-east of Korea. The UHRS is constructed for the mean annual frequency of exceedance of 1.0E-4 using only area sources (KAERI, 2012). The ground motion prediction equation of Atkinson and Boore (2006) is adopted considering low-to-moderate seismicity of Korea located in stable continental region. Site condition of $V_{s30} = 760m/s$ is assumed. The UHRS of the site and the certified seismic design response spectrum (CSDRS) for APR 1400 NPP are compared in Figure 2. The UHRS is much lower than the CSDRS for most frequencies except for 20 to 50 Hz where the UHRS is comparable to the CSDRS.

EARTHQUAKE SCENARIO BASED ON DEAGGREGATION

Deaggregation of the seismic hazards is performed at control frequencies to be used for CMS. The first and second modal frequencies are adopted. In addition, two thirds of the first modal frequency is adopted as an additional control frequency considering stiffness decrease due to nonlinear behaviour of the structure. Deaggregation of the UHRS for selected control frequencies was performed and the results are represented in Figure 3. It is observed that the bin corresponding to epicentral distance from 0 to 20 km and magnitude from 6.2 to 6.4 contributes the most to seismic hazards at the site for all three control frequencies. However, no single bin makes prominent contribution and contribution from other scenarios is not negligible. Therefore, it is necessary to consider multiple scenarios in construction of CMS.

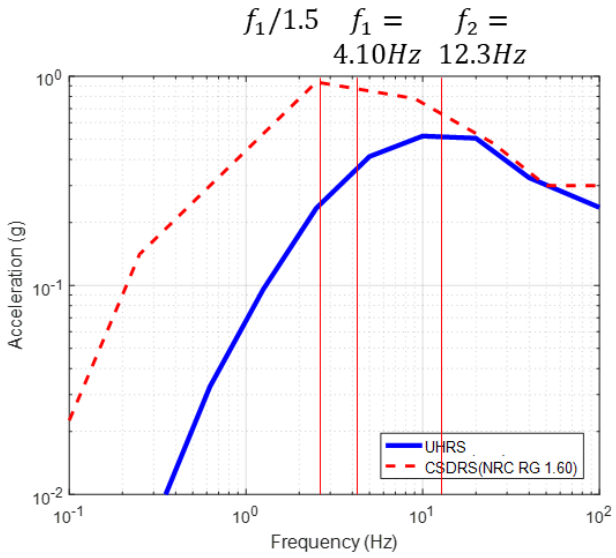

Figure 2. UHRS and CSDRS for the example NPP

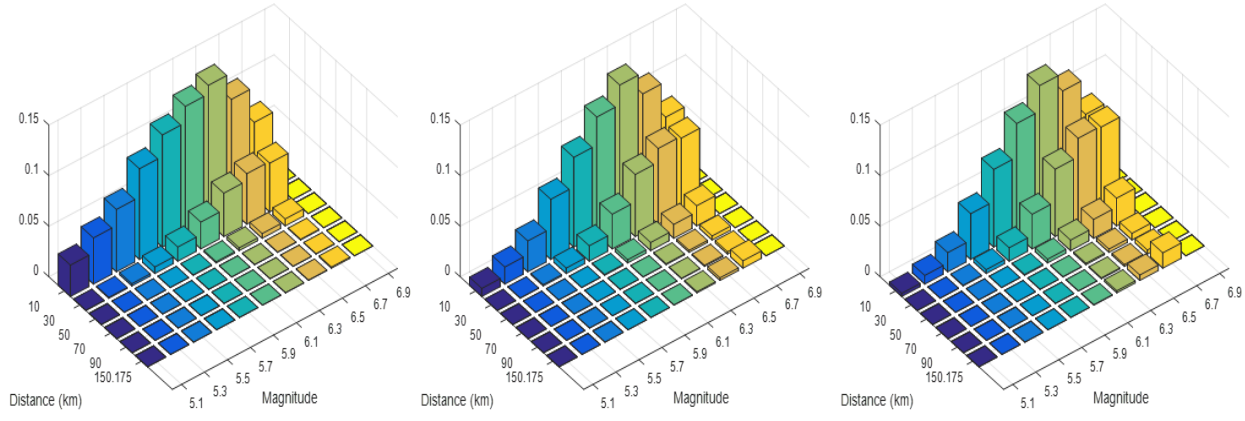

(a) $f_c = f_1/1.5$ (b) $f_c = f_1$ (c) $f_c = f_2$

Figure 3. Deaggregation of UHRS at each control frequency

MULTI-SCENARIO CONDITIONAL MEAN SPECTRUM

For each control frequency, 14 to 15 scenarios with contribution more than 1% are chosen from the result of deaggregation. CMS is constructed for each scenario. An example of CMS computed with the control frequency equal to the first modal frequency is plotted in Figure 4, which plots median conditional spectrum (CS), 2.5 and 97.5 percentile CS, and 30 spectra simulating the probability distribution of the CS obtained by the computer code by Jayaram et al. (2011).

CMS with $f_c = f_1$ are plotted for 15 scenarios in Figure 5, where the CMS with the highest contribution is highlighted with a thick solid line. In addition, weighted average of the CMS and UHRS are plotted for comparison in Figure 5. The highest contributing CMS is higher than the UHRS at frequencies higher than 10 Hz. However, the weighted average CMS is considerably lower than the UHRS, which indicate that the highest contribution scenario is not sufficiently dominant.

The multi-scenario conditional mean spectrum (MCMS) is defined as the weighted average spectra based on deaggregation. MCMS for three different control frequencies and UHRS are compared in Figure 6. All MCMS are lower than the UHRS except at their own control frequency.

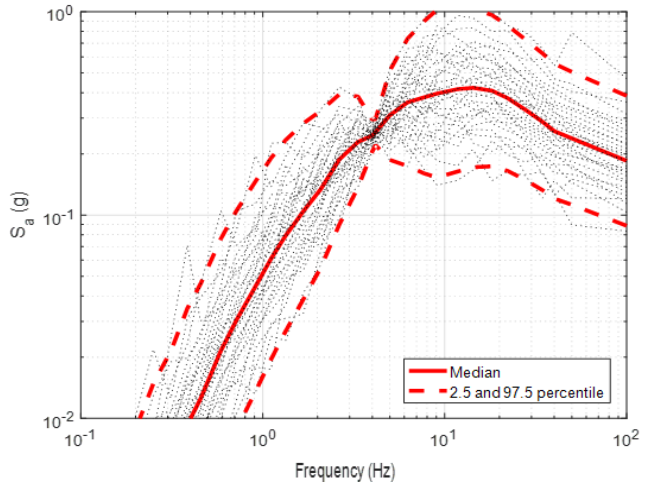

Figure 4. Conditional spectrum for $f_c = f_1$

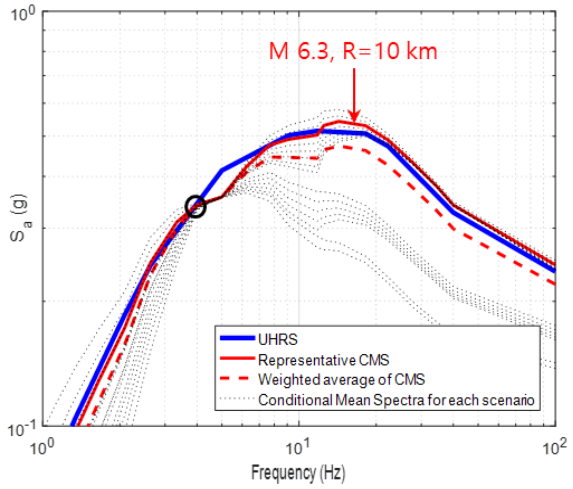

Figure 5. CMS for each scenario and weighted average ($f_c = f_1$)

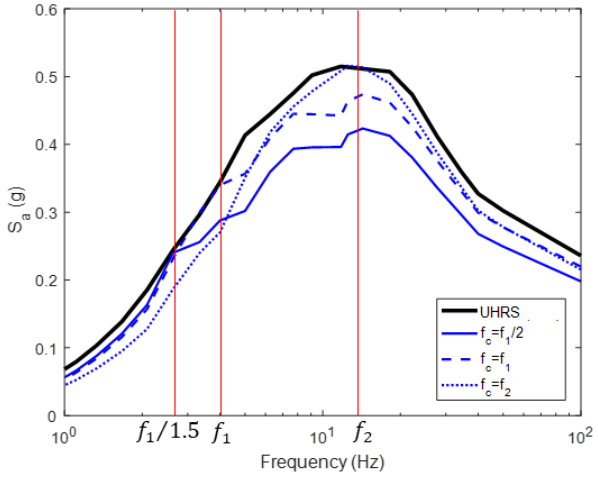

Figure 6. MCMS for different control frequencies

Table 2. Base shear and overturning moment (parenthesis is the reduction ratio compared to UHRS)

Spectrum	UHRS	MCMS1	MCMS2	MCMS3
Base shear (kN)	85,434	65,027 (-23.9%)	76,919 (-10%)	68,228 (-20.1%)
Overturning moment (kN-m)	3.82×10^6	2.91×10^6 (-23.8%)	3.47×10^6 (-9.2%)	2.93×10^6 (-23.2%)

Base shears and overturning moments of the containment structure calculated based on UHRS and MCMS are summarized in Table 2. MCMS for the control frequency of $f_1/1.5$, f_1, and f_2 are denoted by MCMS1, MCMS2 and MCMS3, respectively. MCMS show 10 to 20% reduction of base shear compared to UHRS. In particular MCMS1 with $f_c = f_1$ shows the smallest reduction of seismic load.

SEISMIC FRAGILITY ANSLYSIS

Seismic fragility of the containment structure is assessed using response spectrum analysis in accordance with TR-103959 (Reed and Kennedy, 1994). The median 5-percent damped average spectral acceleration capacity is a spectral acceleration corresponding to the strength of the structure increased by inelastic energy absorption as defined by Equation (1).

$$\bar{S}_a = F_S F_\mu S_a \tag{1}$$

where F_S is the strength factor or the median elastic scale factor required to scale a reference earthquake to reach the elastic structural capacity, F_μ is the median inelastic energy absorption factor, S_a is the reference linear elastic seismic demand. The strength factor and the median inelastic energy absorption factor are defined by Equation (2) and (4), respectively.

$$F_s = \frac{C - D_{NS}}{D_s + \Delta C_s} \tag{2}$$

where D_s is the reference linear elastic seismic demand, , C is the median capacity, ΔC_s is the reduction in capacity due to concurrent seismic loadings, D_{NS} is the concurrent non-seismic demand. The median inelastic energy absorption factor. Internal pressure and vertical component of ground motions are not taken into account so that D_s and ΔC_s is assumed to be 0 in this study.

The inelastic energy absorption factor is calculated by the effective frequency/effective damping method on the basis of ductility factor defined by Equation (3).

$$\mu = \frac{\sum W_i \delta_{T_i}}{\sum W_i \delta_{e_i}} \tag{3}$$

where W_i is the i-th level weight, δ_{T_i} is the median peak displacement at the i-th level, δ_{e_i} is the median peak displacement of the i-the level scaled to yield in the critical level. The drift 0.0075 is adopted as a median peak displacement at the critical level to define the limit state of the containment structure. The bottom element of the beam-stick model is adopted for the critical part of the structure. The ultimate strength of the containment structure is based on the tangential shear strength for cylindrical concrete walls (Ogaki et al., 1981). Yield strength of the containment structure is determined using the concrete part of the prestressed containment structure (ASME, 2015). Limit state caused by flexural failure is minor and excluded in this study. The inelastic energy absorption factor is calculated by Equation (4).

$$F_\mu = \left(\frac{f_e/f}{f_s/f}\right)^2 \frac{S_a(f,\beta)}{S_a(f_e,\beta_e)} \quad (4)$$

where f_s/f is the ratio of the secant frequency and elastic frequency, f_e/f is the ratio of the effective frequency and elastic frequency, $S_a(f,\beta)$ is the spectral acceleration based on the elastic frequency and damping ratio and, $S_a(f_e,\beta_e)$ is the spectral acceleration based on the effective frequency and effective damping ratio.

LOGARITHMIC STANDARD DEVIATION

Logarithmic standard deviations to account for randomness and uncertainty of diverse parameters related to seismic demand and capacity are evaluated for the containment structure. Logarithmic standard deviations for the demand and capacity parameters considered in the study are listed in Table 3 and 4. In addition, logarithmic deviations of the resultant $\bar{S}_a$ are summarized for each spectrum in Table 3 and 4, where β_r and β_u denote logarithmic standard deviations for randomness and uncertainty, respectively. It is noted that response β_r for UHRS is calculated based on demand parameter β_r = 0.20 in accordance with EPRI TR-103959 (Reed and Kennedy, 1994) but β_r's for MCMS are determined by response spectrum analysis for 14 to 15 scenarios, of which each one is composed of 30 simulated spectra respectively, and combining weightings for scenarios obtained from deaggregation results. Vertical component response and relevant demand parameter uncertainties are neglected according to the assumption in modelling. Randomness and uncertainty of the model for capacity parameters are evaluated using Equation (5) and (6), respectively (Reed and Kennedy, 1994).

$$\beta_r = 0.4[0.06 + 0.03(F_\mu - 1)] \quad (5)$$

$$\beta_u = C_u[(F_\mu - 1)] \quad (6)$$

where C_u is between 0.05 and 0.2 usually and 0.1 is adopted in this study.

Among demand parameters, the earthquake response spectrum shape is the most influential parameter except for MCMS2, for which β_u due to frequency uncertainty is higher than all the other spectra. Capacity parameters have smaller variation of logarithmic standard deviation among different spectra than demand parameters comparing Table 3 and 4. Combined logarithmic standard deviations are summarized in Figure 7. The combined logarithmic standard deviation for MCMS2 is similar to UHRS but other MCMS shows considerable increase of standard deviation.

SEISMIC FRAGILITY ASSESSMENT RESULT

Median and HCLPF capacities for different response spectra are summarised in Table 5. The HCLPF capacity represents seismic capacity with 5% probability of failure at 95% confidence level. It is noted that the spectral acceleration capacity is calculated at each control frequency for comparison between UHRS and MCMS, because UHRS and MCMS are the same at the control frequency of MCMS. Among three conditional spectra, MCMS3 shows the highest increase rate of median capacity. However, MCMS3 has the highest combined logarithmic standard deviation too, as shown in Figure 7. As a result, HCLPF spectral acceleration capacity of MCMS2 shows the highest increase rate of 34%. This is because MCMS2 has the lowest logarithmic standard deviation due to zero randomness of spectral shape at the fundamental frequency of the structure. Therefore, the dominant modal frequency is recommended for fragility analysis of a structure of which seismic response is dominated by a single mode such as a containment structure of this case study.

Table 3. Logarithmic standard deviations for demand parameters

Demand parameter			$\bar{S}_a$							
			UHRS		MCMS1		MCMS2		MCMS3	
Parameter	β_r	β_u	β_r	β_u	β_r	β_u	β_r	β_u	β_r	β_u
Earthquake response spectrum shape	0.20	-	0.20	-	0.29	-	0.13	-	0.40	-
Horizontal direction peak response	0.12	-	0.10	-	0.10	-	0.10	-	0.10	-
Damping	-	0.05	-	0.03	-	0.02	-	0.03	-	0.03
Frequency	-	0.05	-	0.11	-	0.08	-	0.14	-	0.08
Mode shape	-	0.15	-	0.15	-	0.15	-	0.15	-	0.15
Torsion coupling	-	0.05	-	0.05	-	0.05	-	0.05	-	0.05
Mode combination	0.10	-	0.10	-	0.10	-	0.10	-	0.10	-
Time history analysis	-	0.05	-	0.05	-	0.05	-	0.05	-	0.05
Ground motion incoherence	-	0.05	-	0.05	-	0.05	-	0.05	-	0.05
SSI analysis	-	0.05	-	0.05	-	0.05	-	0.05	-	0.05
Combined (SRSS)	-	-	0.25	0.21	0.33	0.20	0.19	0.23	0.42	0.20

Table 4. Logarithmic standard deviations for capacity parameters

Demand parameter			$\bar{S}_a$							
			UHRS		MCMS1		MCMS2		MCMS3	
Parameter	β_r	β_u	β_r	β_u	β_r	β_u	β_r	β_u	β_r	β_u
Concrete compressive stress (including aging)	-	0.06 (0.10)	-	0.01	-	0.01	-	0.02	-	0.01
Steel reinforcement	-	0.10	-	0.07	-	0.06	-	0.07	-	0.07
Shear equation	-	0.20	-	0.09	-	0.08	-	0.09	-	0.09
Flexure equation	-	0.15	-	-	-	-	-	-	-	-
Model	Eq. (4)	Eq. (5)	0.04	0.16	0.04	0.15	0.05	0.21	0.05	0.20
Drift	0.15	0.30	0.08	0.15	0.07	0.14	0.08	0.16	0.08	0.15
Combined (SRSS)	-	-	0.09	0.25	0.08	0.23	0.09	0.29	0.09	0.28

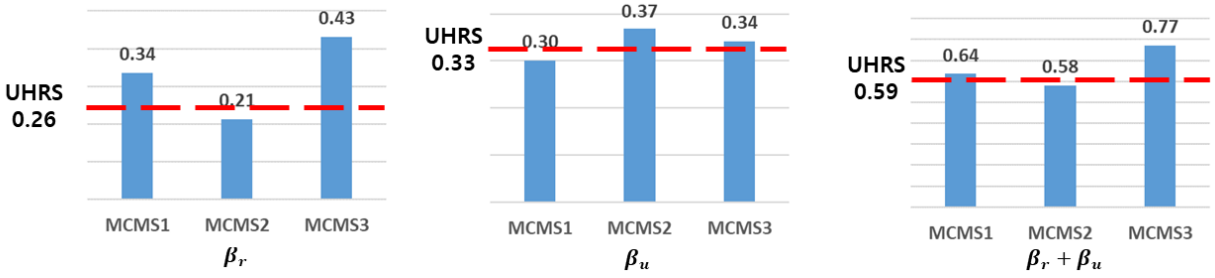

Figure 7. Combined logarithmic standard deviation of spectral acceleration capacity

Table 5. Median and HCLPF spectral acceleration capacities

Control frequency f_c			$f_1/1.5$	f_1	f_2
$S_a(f_c)$ (g)			0.242	0.342	0.514
Median	Spectral acceleration (g)	UHRS (A)	4.52	6.39	9.61
		MCMS (B)	5.75	8.49	14.24
	Rate	$\{(B)-(A)\}/(A)\times 100$ (%)	27	33	48
$HCLPF_{50}$	Spectral acceleration (g)	UHRS (C)	1.72	2.43	3.65
		MCMS (D)	2.02	3.26	3.98
	Rate	$\{(D)-(C)\}/(C)\times 100$ (%)	17	34	9

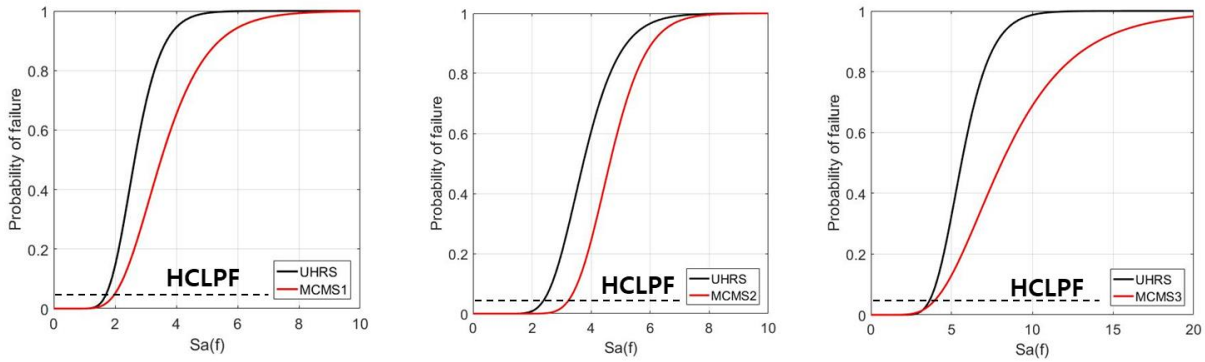

(a) $f = f_1/1.5$ (b) $f = f_1$ (c) $f = f_2$

Figure 8. Fragility curve for different response spectra

Seismic fragility curves for different spectra are plotted in Figure 8. Probabilities of failure for MCMS1 and MCMS3 are similar to those for UHRS at low spectral acceleration capacity but gap between the two curves increases for higher spectral accelerations. However, fragility curves for UHRS and MCMS2 are almost parallel so that both median and HCLPF capacities increases by applying MCMS2, of which control frequency is close to the fundamental frequency of the containment structure.

CONCLUSIONS

A methodology to assess seismic fragility of NPP using MCMS combining multiple scenarios from deaggregation of seismic hazards was proposed in this study. As a validation example, MCMS are constructed for a NPP site and applied to seismic fragility assessment of a containment structure in comparison with using conventional UHRS. Findings from this study are summarized as follows.

1) MCMS is lower than the CMS for the single maximum contribution scenario. Therefore, contribution of multiple scenarios needs to be taken into account unless a single scenario is dominant.
2) Elastic response spectrum analysis of the containment structure using MCMS for multiple scenarios results in 10 to 20% decrease of base shear. The control frequency equal to the fundamental frequency shows the least decrease of base shear.
3) HCLPF capacities based on MCMS for multiple scenarios are improved by 10 to 30% compared to UHRS. Most improvement of HCLPF capacity is achieved by improvement of median capacity because combined logarithmic uncertainty is not reduced by using MCMS.

4) Increase of HCLPF by using MCMS depends on control frequency. Dominant modal frequency is recommended for control frequency in order to reduce the effect of randomness in spectral shape.

ACKNOWLEDGEMENT

This work was supported by the Korea Institute of Energy Technology Evaluation and Planning(KETEP) and the Ministry of Trade, Industry & Energy(MOTIE) of the Republic of Korea (No. 20171510101960).

REFERENCES

ASME. (2015). Boiler and pressure Vessel code, Division 2, Code for Concrete Containments

Atkinson, G. M., Boore, D. M. (2006). "Earthquake Ground-Motion Prediction Equations for Eastern North America", Bulletin of the Seismological Society of America, 96(6), 2181–2205.

Baker, J. W. (2011). "Conditional Mean Spectrum: Tool for Ground-Motion Selection", Journal of Structural Engineering, 137(3), 322-331.

Choi, I-K., Seo, J-M. (2001). "Inelastic Energy Absorption Factor for the Seismic Probabilistic Risk Assessment of NPP Containment Structure," Earthquake Engineering Society of Korea

Jayaram, N., Lin T., Baker J. W. (2011). "A Computationally Efficient Ground-Motion Selection Algorithm for Matching a Target Response Spectrum Mean and Variance," Earthquake Spectra, 27(3), 797-815

Korea Atomic Energy Research Institute (2012). *Development of Ground Response Spectrum for Seismic Risk Assessment,* Republic of Korea.

Korea Electrical Power Corporation, Korea Hydro & Nuclear Power Co., LTD (2014). *APR1400 DESIGN CONTROL DOCUMENT TIER2", APR1400-K-X-FS-14002-NP REVISION 0*, Republic of Korea.

Ogaki, Y., Kobayashi, M., Takeda, T., Yamaguchi, T., Yoshizaki, K., and sugano, S.(1981). "Shear strength tests of prestressed concrete containment vessels," SMiRT-6, J4/3

Reed, J. W., & Kennedy, R. P. (1994). *Methodology for developing seismic fragilities*, EPRI TR-103959. Electric Power Research Institute, Palo Alto, CA.

Renault, P. (2011). "PEGASOS refinement project: new findings and challenges from a PSHA for Swiss Nuclear Power Plants," Transactions, SMiRT 21, Div-IV: Paper ID# 561.